INF5490 RF MEMS

LN06: RF MEMS switches, II

Spring 2009, Oddvar Søråsen

Department of Informatics, UoO

Today's lecture

- Design of RF MEMS switches
  - Electromechanical design, II
  - RF design
- Examples of implementations
  - Structure
  - Fabrication
  - Performance
- Special structures and actuation mechanisms
- Some challenges

Electromechanical design, II

- Designer should take into account

  - **Stress →**

  - Dynamics
    - Damping
    - How actuation voltage influences switch speed

Stress

- Stress induced during fabrication: high T → low T
  - Due to dissimilar properties of neighboring materials
    - "Residual stress"
- Change of stress during operation due to temperature variations
  - Dissimilar CTEs (Coefficient of Thermal Expansion)

- Ex. axial **tensile stress**
  - Spring constant k_z increases
  - k_z increases 20x when tensile stress 0 → 300 MPa
  - Vpi increases 4.5x when tensile stress 0 → 300 MPa
- Tensile stress must be taken into account!
- Stress can be **evaluated** by misalignment measurements on test structures →
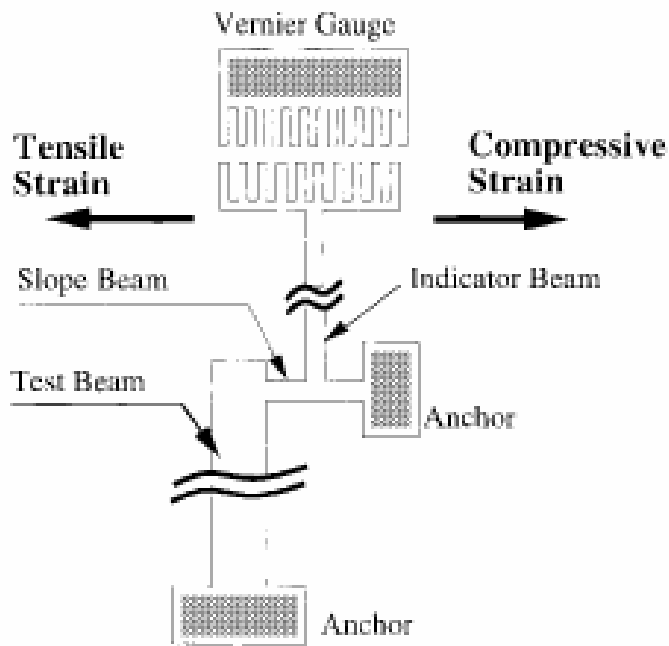
Micro strain gauge with mechanical amplifier

Vernier Gauge

Tensile
Strain

Compressive
Strain

Slope Beam

Indicator Beam

Test Beam

Anchor

Anchor

Fig. 1. Schematic diagram of a strain gauge based on the mechanical amplifier.

Best match
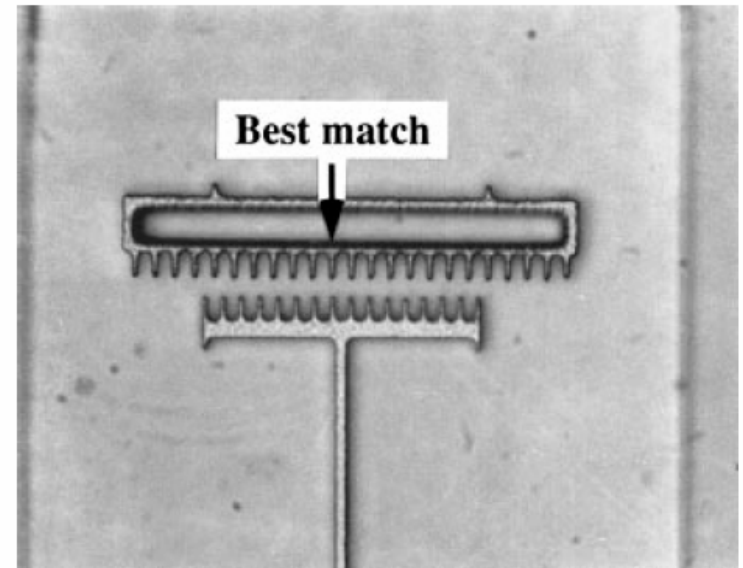
Fig. 4. An example of strain-gauge reading under an optical microscope.

Jmfr. "skyvelær"

Lin et al, J of MEMS, 1997

Switch speed and damping

- Switch speed depends of **damping**
  - Air, gas must be pushed/pulled away
  - **"squeezed-film damping"**
  - Method of modeling from fluid dynamics
- How to reduce damping?
  - Operate in vacuum
    - Hermetic sealed packages
  - Make holes in membrane
    - Perforated membrane →

Perforated membrane: UMICH

Anchor
Folded suspension beams
Center capacitive area
Inductive connecting beams
Pull-down electrode

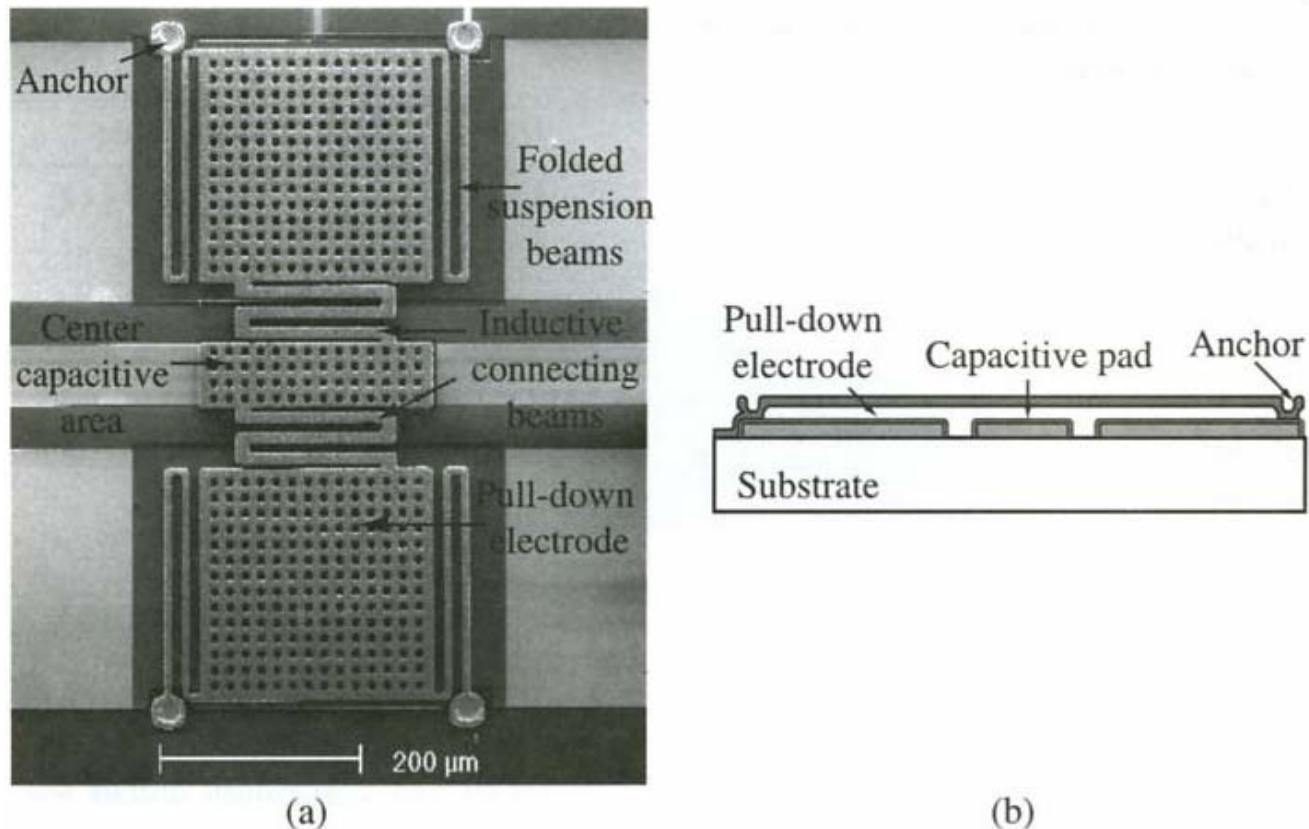Pull-down electrode   Capacitive pad   Anchor
Substrate

200 µm

(a)

(b)

Figure 5.2. Photomicrograph of the university of Michigan low-voltage MEMS shunt switch. The number of meanders can be varied from 1 to 8 [7] (Copyright IEEE).
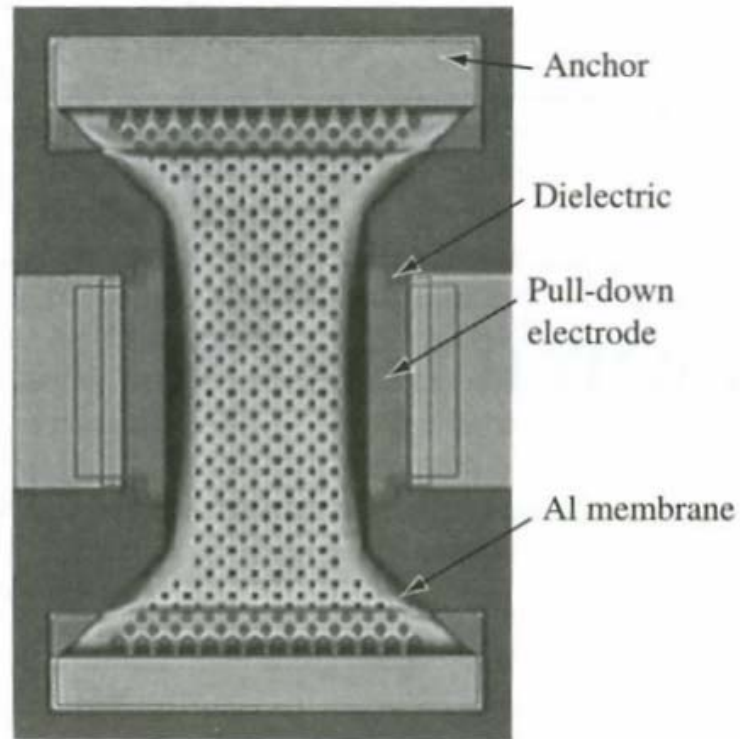
Perforated membrane: Raytheon

Figure 5.1. Photomicrograph of Raytheon MEMS capacitive shunt switch [2, 3] (Copyright IEEE).

Rebeiz

Ex. On effect of perforation

→ Significant increased speed by use of perforated membrane!

	No holes	With holes
b	1.3×10^{-3} Pa.s	2.1×10^{-6} Pa.s
τ_{sdown}	$80\mu S$	$10.5\mu s$

S. Pacheco, L.Katehi, Chapter in 'RF Technologies for Low Power Wireless Communications', Wiley, 2001.
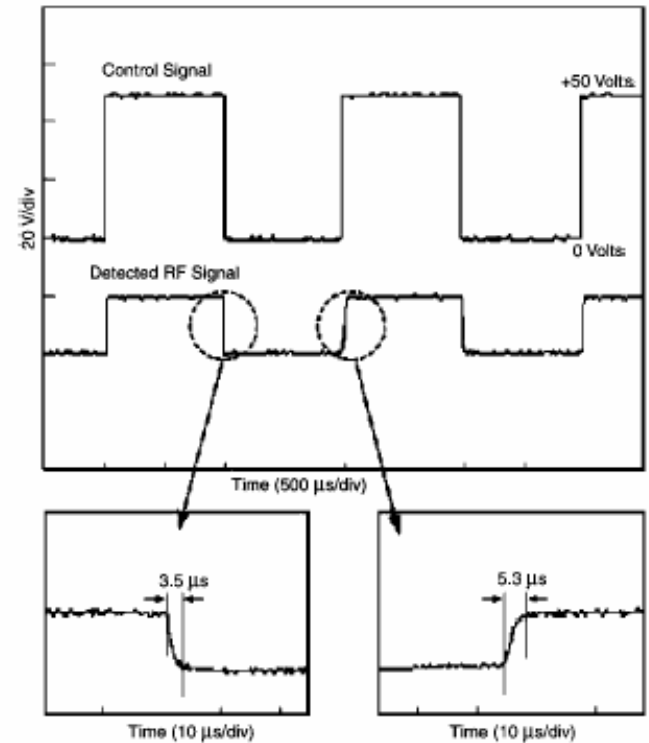
Z.

Figure 12. Switching time of the TI capacitive coupling shunt switch is of the order of 3.5–5.3 μs (from [30], Raytheon/TI).

Switch time for Raytheon/TI-switch

Yao, 2000

9

Switch speed

- Damping influences Q-factor
- Switch-speed depends of Q-factor

  - High Q-factor means small damping
    - $\rightarrow$ increased switch speed
  - Low Q-factor means large damping
    - System is **damping-limited** when Q ≤ 0.5
      [Castaner and Senturia]
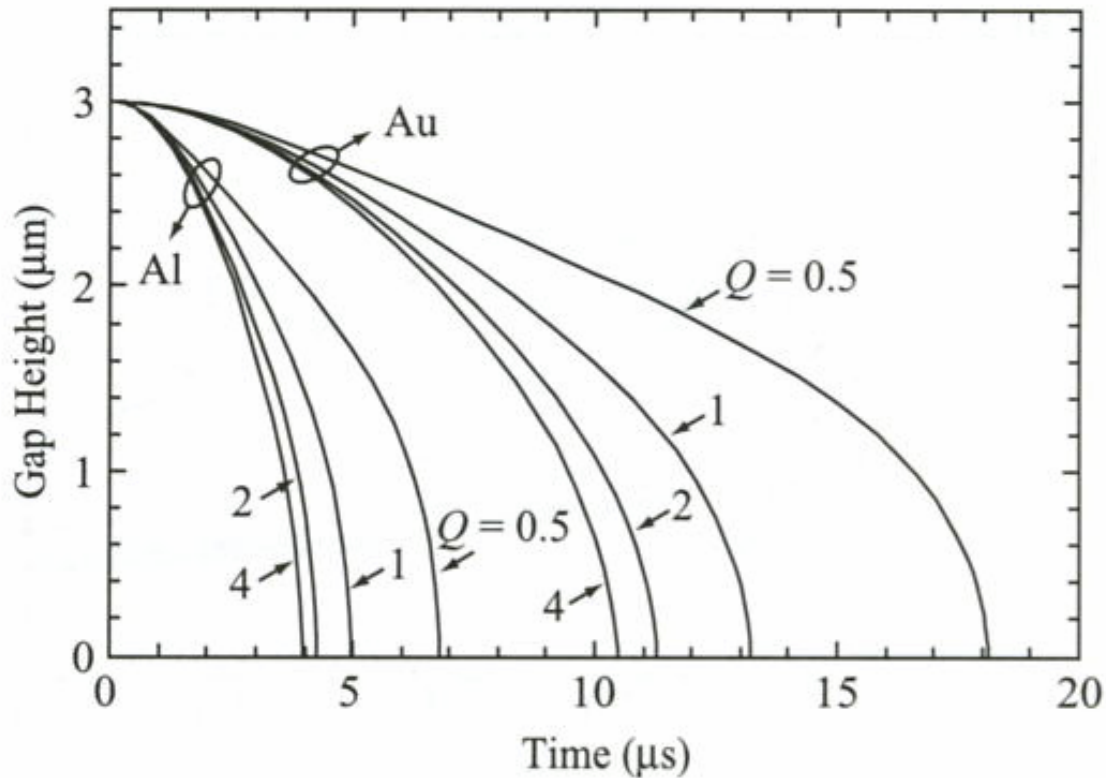
Gap vs. Time for various Q-factors

Figure 3.3. Pull-down simulations for the Au and Al beams of Table 3.1 for an applied voltage of 42 V ($V_s = 1.4V_p$).

(For differences between Al and Au: later →)

Gas damping

Dynamic response of cantilever beam

$$m \frac{d^2 w}{dt^2} + b \frac{dw}{dt} + k \cdot w = F_{ext}$$
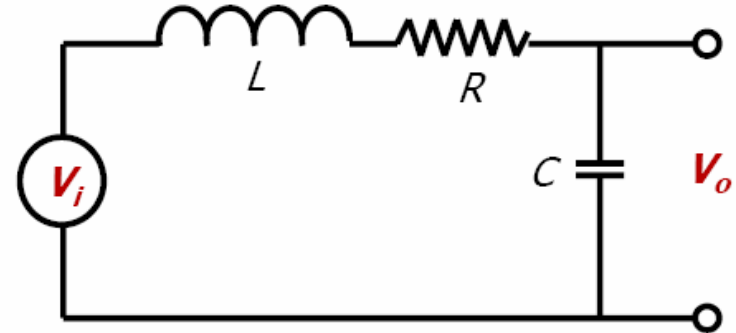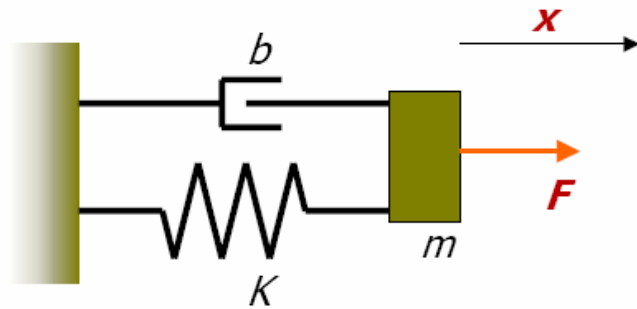
w = displacement
m = mass
b = damping coefficient
k = spring constant

$$\frac{W(j\omega)}{F(j\omega)} = \frac{1}{k} \frac{1}{1 - \left(\frac{\omega}{\omega_0}\right)^2 + j\omega/(Q \omega_0)}$$

$$\omega_0 = \sqrt{\frac{k}{m}} = \quad \text{Resonance frequency}$$

$$Q = k/(\omega_0 b) = \quad \text{Q-factor} \qquad \boxed{Q = (\omega_0 \, m)/b}$$

Mechanical / Electrical Systems

Input : external force F

Output : displacement x

$$m\ddot{x}(t) + b\dot{x}(t) + Kx(t) = F$$

m mass, b damping, K stiffness

Transfer function :

$$H(s) = \frac{x}{F} = \frac{\frac{1}{m}}{s^2 + \frac{b}{m}s + \frac{K}{m}}$$

Input : voltage V_i

Output : voltage V_o

$$L\ddot{q}(t) + R\dot{q}(t) + \frac{1}{C}q(t) = V_i$$

L induct., R resist., C capacit.

Transfer function :

$$H(s) = \frac{V_o}{V_i} = \frac{\frac{1}{LC}}{s^2 + \frac{R}{L}s + \frac{1}{LC}}$$

Resonators

- Analogy between mechanical and electrical system:
  - Mass m - inductivity L
  - Spring K - capacitance C
  - Damping b - resistance R (depending where R is placed in circuit)

- Solution to 2nd order differential equation:

$$H(s) = \frac{\omega_0^2}{s^2 + \frac{\omega_0}{Q}s + \omega_0^2}$$

$$\omega_0 = 2\pi f_0 \quad \text{natural frequency}$$

$$\omega_0 = \sqrt{\frac{K}{m}} \text{ mechanical system,} \quad \omega_0 = \sqrt{\frac{1}{LC}} \text{ electrical system}$$

$$Q \quad \text{quality factor}$$

m for gas damping

- Q depends on the relationship between **m, b, k**
  - m is **"effective mass"** ("dynamic mass")
    - The effective mass is different from the physical mass since only the end/central part of the cantilever/beam is moving
    - m_eff ~ 0.35 – 0.45 *m_total
    - m_eff depends of
      - Topology/ physical dimensions
      - Spring constant, material choice
      - Dynamics
  - Will be calculated more accurately in a future lecture

b for gas-damping

- – Q depends of b = damping coefficient
- – Damping, b, depends of **viscosity**
  - • Viscosity is internal resistance against gas transport
- – Ex.: damping for rectangular parallel plate:

$$b = \frac{3}{2\pi} \cdot \frac{\mu \cdot A^2}{g_0{}^3}$$

$A =$ area $g_0 =$ gap

$\mu =$ viscosity of gas

Q for gas damping

Gas damping influences Q-factor

Quantitative equations:

$$Q = k/(\omega_0 b)$$

$\rho =$ density

$$Q_{cantilever} = \frac{\sqrt{E\rho}\; H^2}{\mu\,(WL)^2}\, g_0^3$$

$$Q_{cc} = $$

$$W \cdot L \longrightarrow \frac{W \cdot L}{2}$$

for clamped-clamped beam

Switch speed for large damping

For a **damping-limited** system

$$(Q \leq 0.5)$$

simplification of equation

Equation of motion

$$b \frac{dw}{dt} = F_{ext}$$

A quantitative expression:

$$t_s \approx \frac{9 V_{Pi}^2}{4 w_o Q V_s^2} \quad \text{for } V_s \gg V_{Pi}$$

Vs = actuation voltage

Rebeiz

18

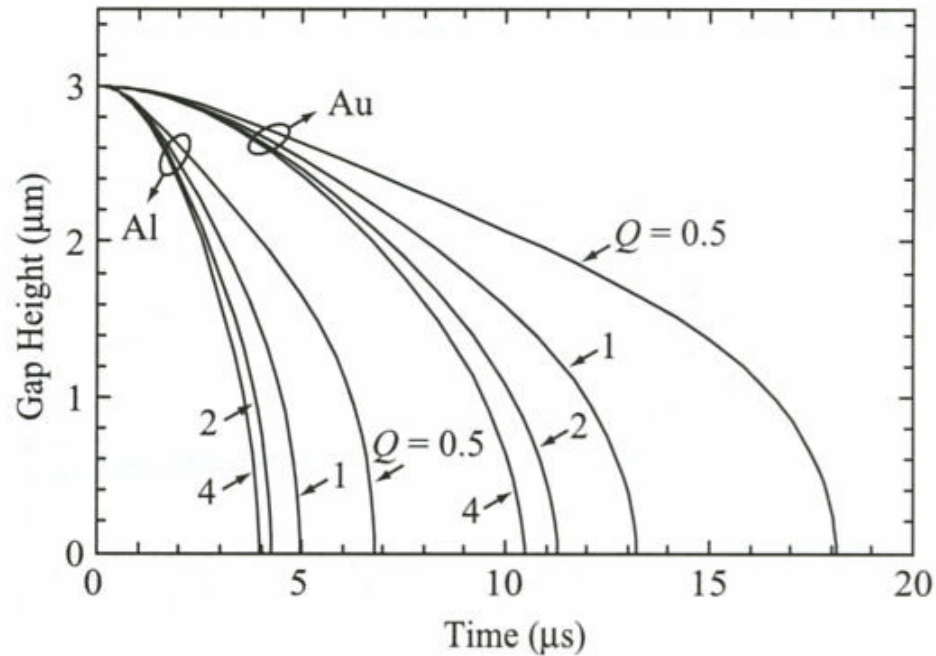# Time response for various Q-factors

Figure 3.3. Pull-down simulations for the Au and Al beams of Table 3.1 for an applied voltage of 42 V ($V_s = 1.4 V_p$).

Note: Au has higher density → larger mass → lower ω → larger switch time (t_s)

Switch speed for increased Vs

- Switch-speed strongly depends of actuation voltage, Vs
  - Vs is usually larger than Vpi
  - Vs = const * Vpi (pull-in) = ("actuation voltage")
  - Larger voltage gives larger electrostatic force
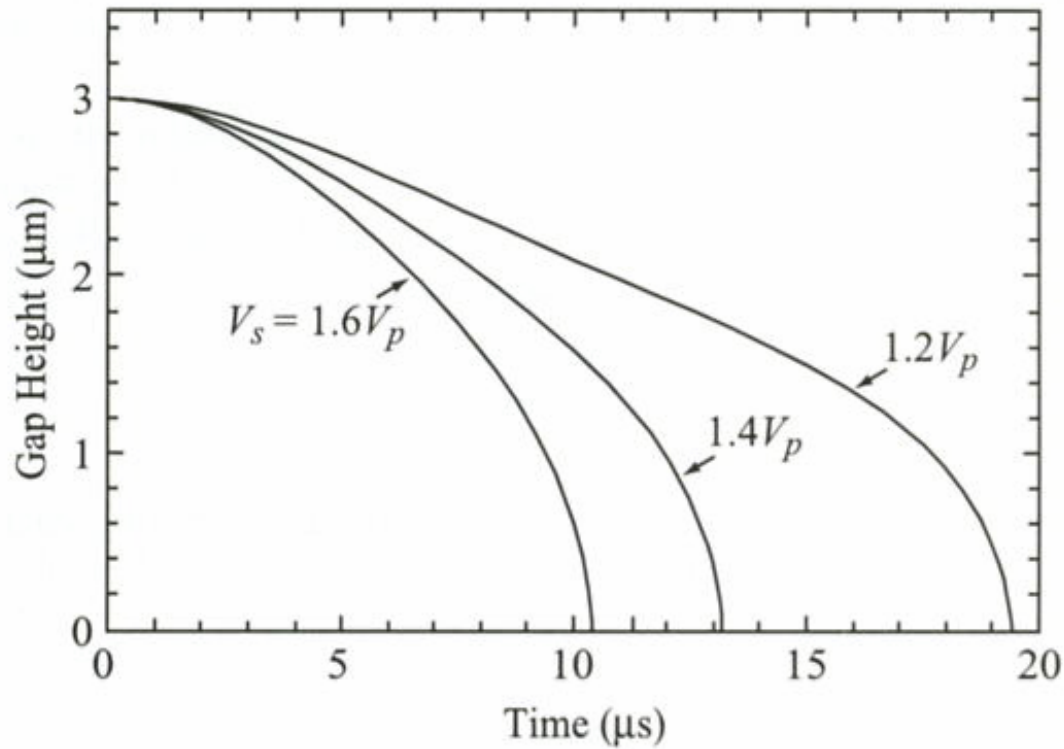   - → increased switch speed

Time response vs. applied voltage

Figure 3.4. Pull-down simulations for the Au beam of Table 3.1 versus the applied voltage, and $Q = 1$.

Switch speed for small damping

Electrostatic force

$$F = \frac{\varepsilon_0 A V^2}{2 g^2}$$

"Acceleration limited" switch (b~0)

$$m \frac{d^2 w}{dt^2} + k \cdot w = -\frac{\varepsilon_0 A V^2}{2 g_0^2} \qquad (Q \geq 2)$$

Actuation voltage

$$V_s = kout \times V_{Pi}$$

Switch time

$$t_s \approx 3.67 \frac{V_{Pi}}{V_s \cdot w_0}$$
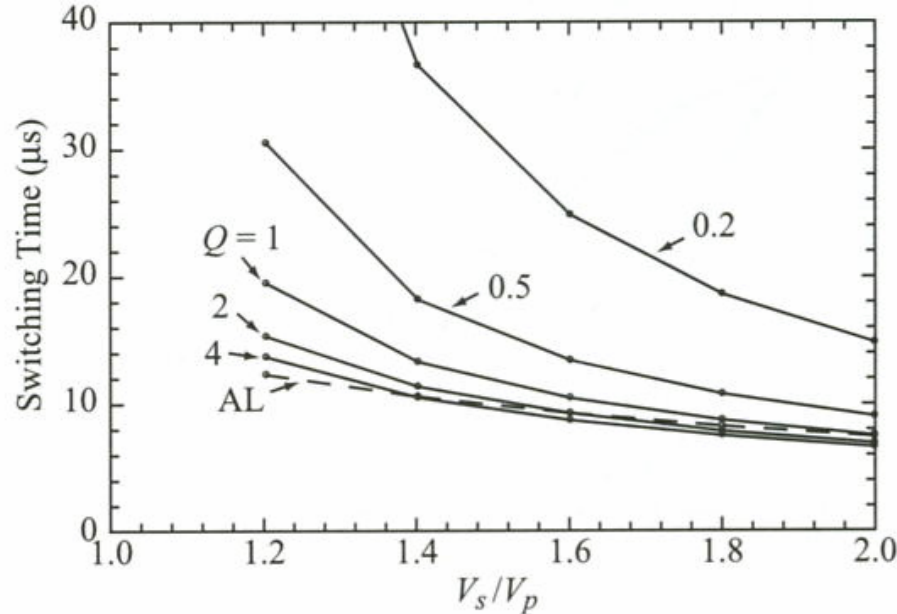
Rebeiz

Acceleration limited switch

Figure 3.5. Simulated switching times for the Au beam given in Table 3.1. "AL" means acceleration-limited and is given by Eq. (3.23).

**Note: The system becomes more acceleration limited when damping decreases (eg. Q-factor increases).
High Vs/Vp is good.**

RF design of MEMS switch

- Detailed **electromagnetic** modeling can be used
  - 3 dim electromagnetic analysis of **field distributions**
    - Detailed mechanical model
    - Depends on material properties, boundary conditions etc.
  - → Calculating field distributions and S-parameters

- Alternatively: use equivalent circuit models →
  - Simple models for analytic calculations
    - Can be used to estimate RF performance

Electrical characterization of RF MEMS switches

- For "low" frequency
  - Use impedance – admittance parameters
    - Two-port with voltage and current (Kirchhoff´s equations)

- For high frequency
  - Use S-parameters
  - S-parameters are measured/calculated when the line is terminated with its characteristic impedance
  - S-parameters are small signal parameters
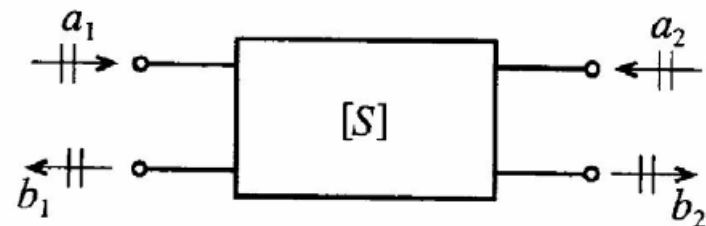   - RF power < DC power
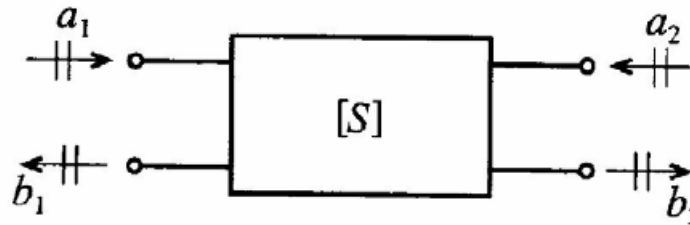
Definition of S-parameters

- Calculating power:

$$P_n = \tfrac{1}{2} \mathrm{Re}\{V_n I_n^*\} = \tfrac{1}{2}\left(\left|a_n\right|^2 - \left|b_n\right|^2\right)$$

S-parameters

$$\begin{Bmatrix} b_1 \\ b_2 \end{Bmatrix} = \begin{bmatrix} S_{11} & S_{12} \\ S_{21} & S_{22} \end{bmatrix} \begin{Bmatrix} a_1 \\ a_2 \end{Bmatrix}$$

Meaning of S-parameters

$$S_{11} = \left.\frac{b_1}{a_1}\right|_{a_2 = 0} \equiv \frac{\text{reflected power wave at port 1}}{\text{incident power wave at port 1}} \qquad (4.42a)$$

$$S_{21} = \left.\frac{b_2}{a_1}\right|_{a_2 = 0} \equiv \frac{\text{transmitted power wave at port 2}}{\text{incident power wave at port 1}} \qquad (4.42b)$$

$$S_{22} = \left.\frac{b_2}{a_2}\right|_{a_1 = 0} \equiv \frac{\text{reflected power wave at port 2}}{\text{incident power wave at port 2}} \qquad (4.42c)$$

$$S_{12} = \left.\frac{b_1}{a_2}\right|_{a_1 = 0} \equiv \frac{\text{transmitted power wave at port 1}}{\text{incident power wave at port 2}} \qquad (4.42d)$$

Measuring S-parameters

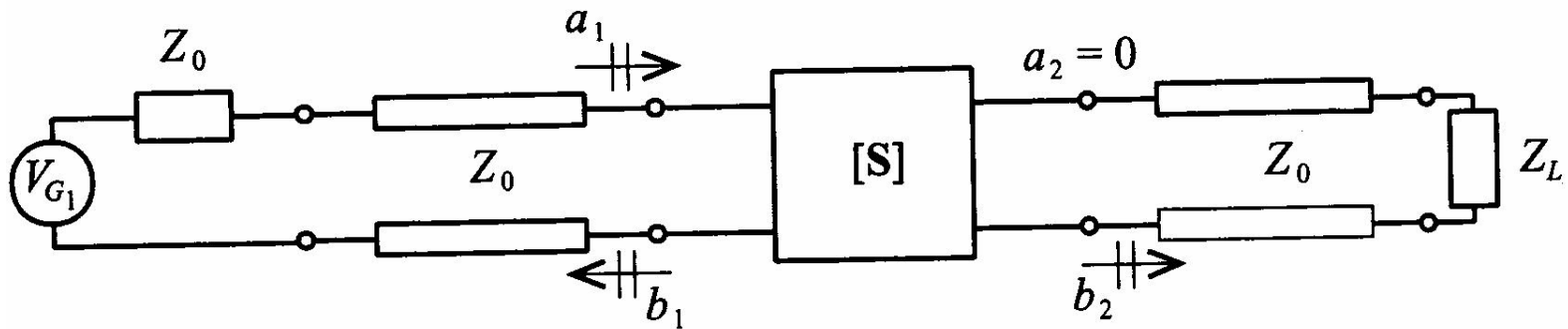- S-parameters measured when lines are **terminated** with **characteristic impedance**

Figure 4-15 Measurement of S_{11} and S_{21} by matching the line impedance Z_0 at port 2 through a corresponding load impedance $Z_L = Z_0$.

RF characterization

- Reflected and transmitted signals should be taken into account

- Important parameters calculated
  - **Insertion loss** in ON-state (down) =
  - **Isolation** i OFF-state (up) =
  - **Return loss** (both up/down) =

RF characterization, contd.

”IL = Insertion loss” i ”on-state”

$$S_{21} = \left.\frac{b_2}{a_1}\right|_{a_2=0} = \frac{transmitted,\,port2}{incident,\,port1}$$

The **inverse** value is used for IL

Specified in dB

Degrades with increased frequency

RF characterization, contd.

"Isolation" in "off-state"

$$\frac{1}{S_{21}} = \frac{a_1}{b_2}\bigg|_{a_2=0} = \frac{incident, port1}{transmitted, port2}$$

(Varadan)

$$\frac{1}{S_{12}} = \frac{a_2}{b_1}\bigg|_{a_1=0} = \frac{incident, port2}{transmitted, port1}$$

(most common def)

→High isolation when output is small relative to input
(or input is marginally influenced by output)

"Return loss" for both states

$$S_{11} = \frac{b_1}{a_1}$$

eg. Large loss for much reflected

S-parameters

- In UP-state: S_{21} is corresponding to **isolation**

- In DOWN-state: S_{21} is corresponding to **insertion loss**

- In UP-state: S_{11} is corresponding to **return loss**

- In DOWN-state: S_{11} is corresponding to **return loss**
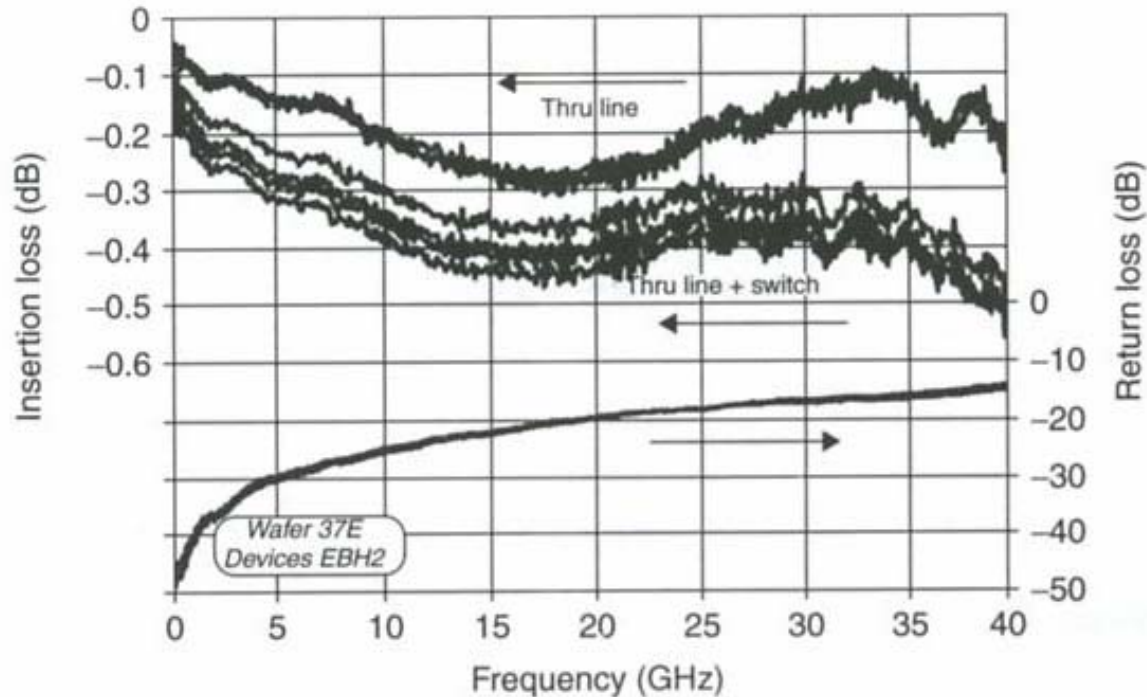
Typical s-parameter measurements

Figure 3.25 Measured insertion loss and return loss RF MEMS switch. Reproduced from C.L. Goldsmith, Z. Yao, S. Eshelman and D. Denniston, 1998, 'Performance of low-loss MEMS capacitive switches', *IEEE MW and Guided wave Letters* **8**(8): 269–271, by permission of IEEE, © 1998 IEEE

Varadan

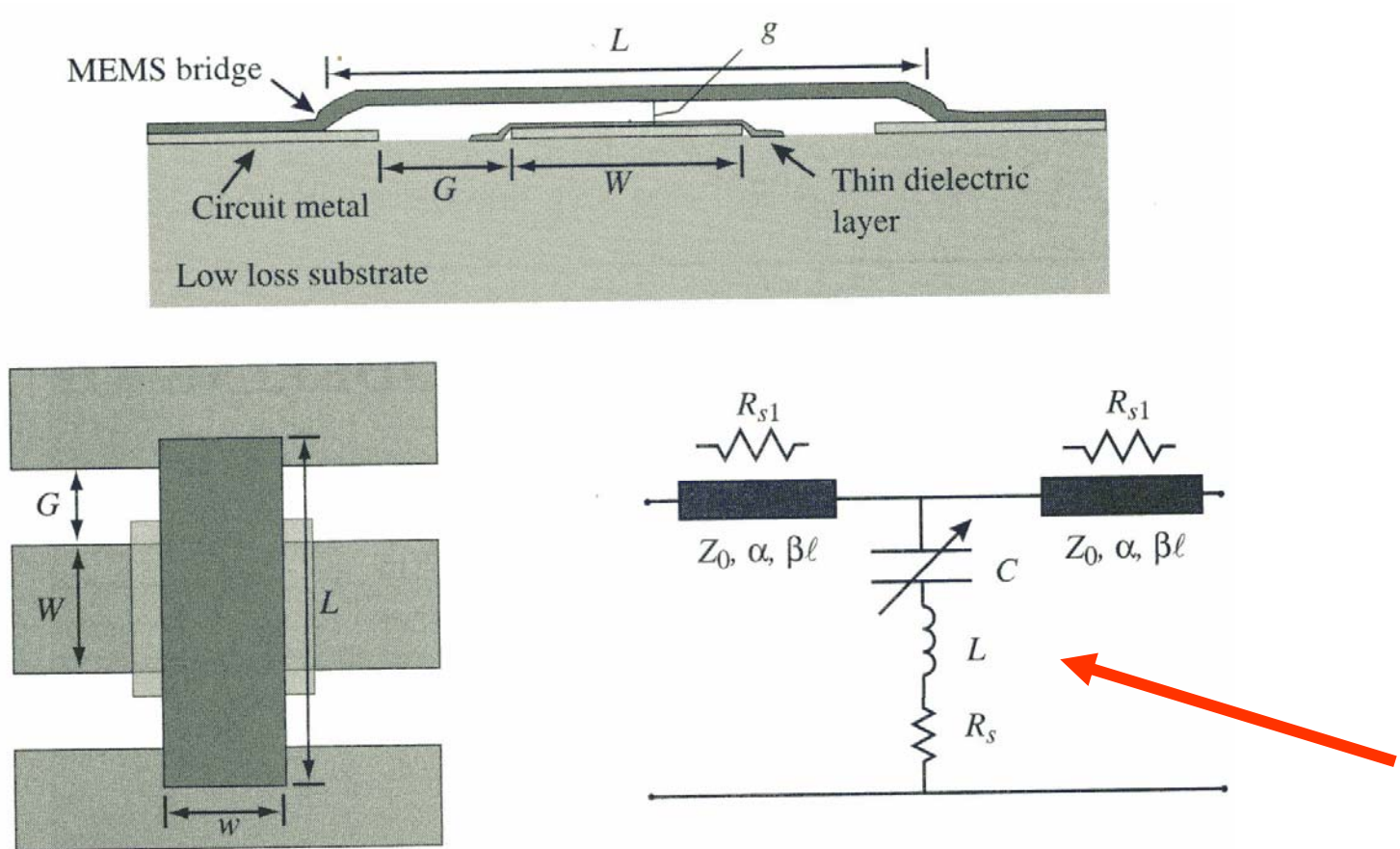# Equivalent circuit for capacitive shunt switch

Figure 4.1. Illustration of a typical MEMS shunt switch shown in cross section and plan view. The equivalent circuit is also shown [6] (Copyright IEEE).

Rebeiz

Equivalent circuit, contd.

Switch shunt impedance

$$Z_s = R_s + j\omega L + \frac{1}{j\omega C}$$

$$C = C_u \ ???u \ C_d$$

At resonance

$$\omega_0 L = \frac{1}{\omega_0 C}$$

$$\omega_0 = \sqrt{\frac{1}{LC}}$$

$$Z_s = \begin{cases} \dfrac{1}{j\omega C} & \text{for } f \ll f_0 \\ R_s & \text{"} \quad f = f_0 \\ j\omega L & \text{"} \quad f \gg f_0 \end{cases}$$

RF parasitics

- Simplified calculations for shunt switch:
  - Use C only
- More accurate calculations:
  - Include L
  - **Meander spring** contributes to parasitics!

  - Meanders give a **softer spring**
    - Give lower Vpi
  - → contribute to **parasitic inductance**
    - → influence RF-performance

- Accurate modeling should take into account parasitic inductance and parasitic resistance
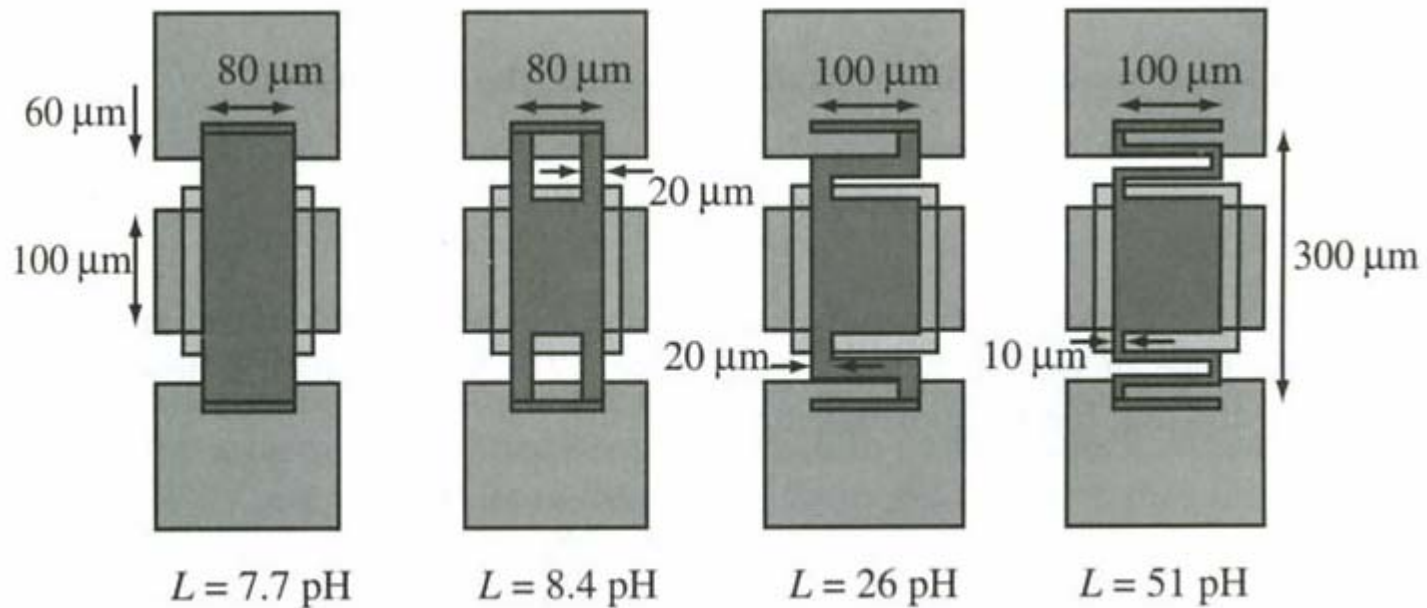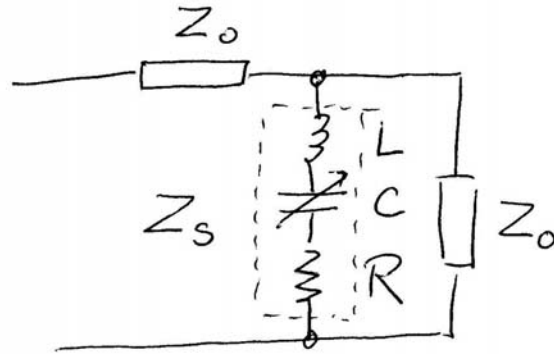
Parasitic inductance

Figure 4.4. Simulated inductance for low-spring-constant MEMS bridges.

Labels on figure:
- $L = 7.7$ pH
- $L = 8.4$ pH
- $L = 26$ pH
- $L = 51$ pH

Dimensions: 80 μm, 60 μm, 100 μm, 20 μm, 10 μm, 300 μm

Meander spring increases inductance

Rebeiz

Shunt configuration

$$Z_s = R + j\omega L + \frac{1}{j\omega C}$$

$$S_{11} = S_{22} = \Gamma = \frac{Z_L - Z_o}{Z_L + Z_o} = \frac{Z_s // Z_o - Z_o}{Z_s // Z_o + Z_o} = \frac{-Z_o}{2Z_s + Z_o}$$

$$S_{12} = S_{21} = 1 + \Gamma = 1 + \frac{-Z_o}{2Z_s + Z_o} = \frac{2Z_s}{2Z_s + Z_o}$$

38

Return loss (up-state)

$$Z_s \approx \frac{1}{j\omega C}$$

$$S_{11} = \frac{-Z_0}{2Z_s + Z_0} = \frac{-Z_0}{2 \cdot \frac{1}{j\omega C} + Z_0} = \frac{-j\omega C Z_0}{2 + j\omega C Z_0}$$

$$|S_{11}|^2 = S_{11} \cdot S_{11}^* = \frac{(\omega C Z_0)^2}{4 + (\omega C Z_0)^2}$$

Return loss (down-state)

$$Z_s = R + j\omega L + \frac{1}{j\omega C}$$

$$S_{11} = \frac{-Z_0}{2Z_s + Z_0} = \frac{-Z_0}{2\left(R + j\omega L + \frac{1}{j\omega C}\right) + Z_0} = \frac{-j\omega C Z_0}{(2 - 2\omega^2 LC) + j\omega(2R + C Z_0)}$$

$$|S_{11}|^2 = S_{11} \cdot S_{11}^* = \frac{(\omega C Z_0)^2}{(2 - 2\omega^2 LC)^2 + (2\omega R + \omega C Z_0)^2}$$
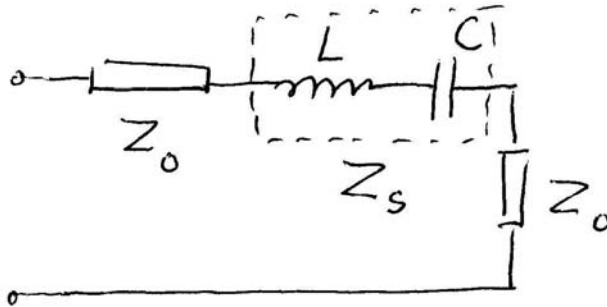
39

$$S_{12} = S_{21} = \frac{2Z_s}{2Z_s + Z_0} = \frac{2\left(R + j\omega L + \frac{1}{j\omega c}\right)}{2\left(R + j\omega L + \frac{1}{j\omega c}\right) + Z_0}$$

$$= \frac{(2 - 2\omega^2 LC) + j2\omega RC}{(2 - 2\omega^2 LC) + j(2\omega RC + \omega C Z_0)}$$

$$|S_{12}|^2 = |S_{21}|^2 = S_{21} * S_{21}^* = \frac{(2 - 2\omega^2 LC)^2 + (2\omega RC)^2}{(2 - 2\omega^2 LC)^2 + (2\omega RC + \omega C Z_0)^2}$$

40

$$Z_s = j\omega L + \frac{1}{j\omega C}$$

$$S_{11} = S_{22} = \Gamma = \frac{Z_L - Z_0}{Z_L + Z_0} = \frac{(Z_s + Z_0) - Z_0}{(Z_s + Z_0) + Z_0} = \frac{Z_s}{2Z_0 + Z_s}$$

$$S_{12} = S_{21} = 1 - \Gamma = 1 - \frac{Z_s}{2Z_0 + Z_s} = \frac{2Z_0}{2Z_0 + Z_s}$$

41

$$S_{11} = S_{22} = \frac{Z_s}{2Z_0 + Z_s} = \frac{jwL + \frac{1}{jwC}}{2Z_0 + \left(jwL + \frac{1}{jwC}\right)} = \frac{1 - w^2 LC}{(1 - w^2 LC) + j 2wCZ_0}$$

$$|S_{11}|^2 = S_{11} \cdot S_{11}^* = \frac{(1 - w^2 LC)^2}{(1 - w^2 LC)^2 + (2wCZ_0)^2} = \frac{1}{1 + (2wCZ_0)^2}$$
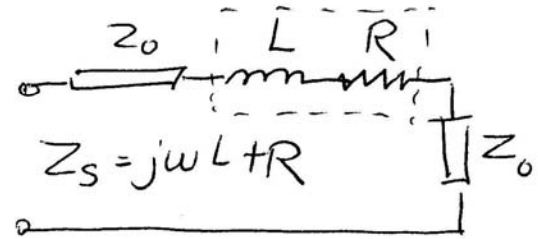
$$\uparrow$$
$$L = 0$$

Isolation (up-state)

$$S_{12} = S_{21} = \frac{2Z_0}{2Z_0 + Z_s} = \frac{2Z_0}{2Z_0 + \left(jwL + \frac{1}{jwC}\right)} = \frac{j 2wCZ_0}{(1 - w^2 LC) + j 2wCZ_0}$$

$$|S_{12}|^2 = S_{12} \cdot S_{12}^* = \frac{(2wCZ_0)^2}{(1 - w^2 LC)^2 + (2wCZ_0)^2} = \frac{(2wCZ_0)^2}{1 + (2wCZ_0)^2}$$

$$\uparrow$$
$$L = 0$$

42

<u>Series switch</u>

<u>Return loss</u> (down-state)

$$Z_S = j\omega L + R$$

$$S_{11} = \frac{Z_S}{2Z_0 + Z_S} = \frac{j\omega L + R}{2Z_0 + j\omega L + R}$$

$$|S_{11}|^2 = S_{11} \cdot S_{11}^* \cdot = \frac{R^2 + (\omega L)^2}{(2Z_0 + R)^2 + (\omega L)^2} \quad \underset{L=0}{=} \quad \frac{R^2}{(2Z_0 + R)^2}$$

<u>insertion loss</u> (down-state)

$$S_{12} = \frac{2Z_0}{2Z_0 + Z_S} = \frac{2Z_0}{2Z_0 + j\omega L + R}$$

$$|S_{12}|^2 = S_{12} \cdot S_{12}^* = \frac{(2Z_0)^2}{(2Z_0 + R)^2 + (\omega L)^2} \quad \underset{L=0}{=} \quad \frac{2Z_0^2}{(2Z_0 + R)^2}$$
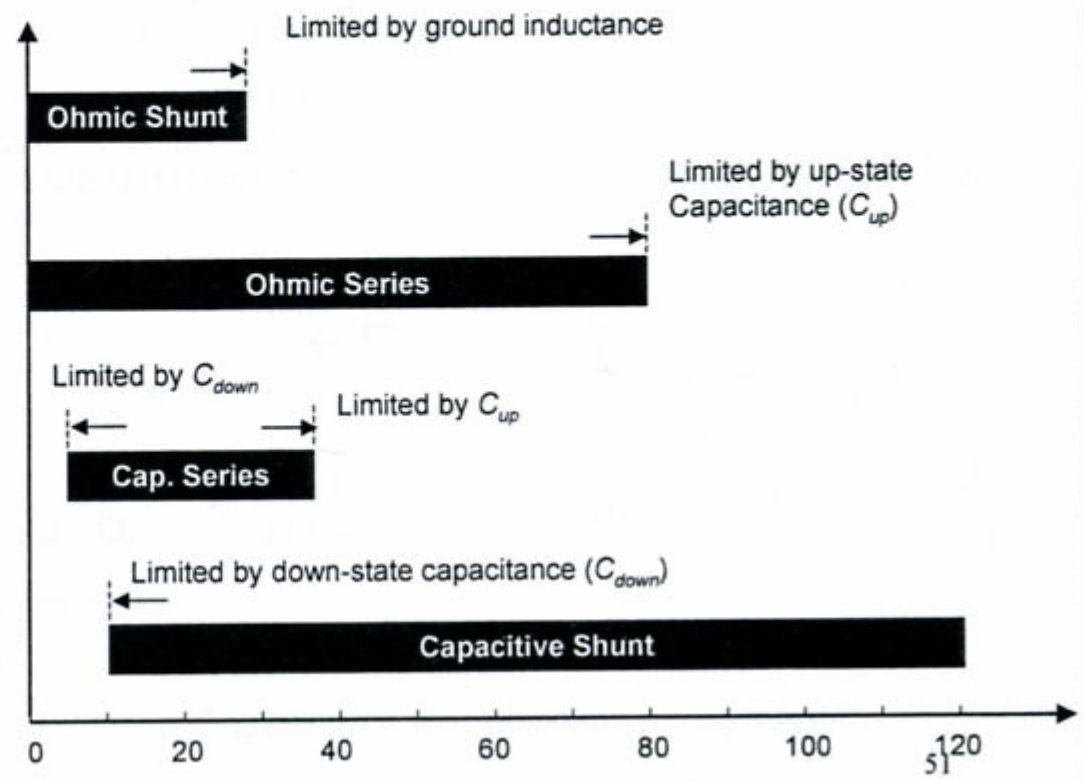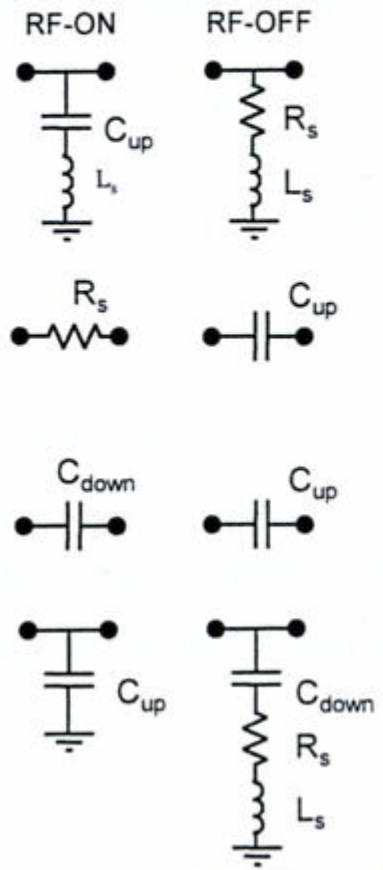
43

RF MEMS switch vs. frequency

Equivalent circuit

G. Rebeiz, "Short course on RF-MEMS", Dec. 2003
H. Tilmans, Microwave week, 2004.

RF-ON   RF-OFF

C_{up} R_s
L_s L_s

R_s C_{up}

C_{down} C_{up}

C_{up} C_{down}
                R_s
                L_s

Limited by ground inductance

Ohmic Shunt

Limited by up-state
Capacitance (C_{up})

Ohmic Series

Limited by C_{down} Limited by C_{up}

Cap. Series

Limited by down-state capacitance (C_{down})

Capacitive Shunt

0   20   40   60   80   100   120

44

Examples of implemented switches
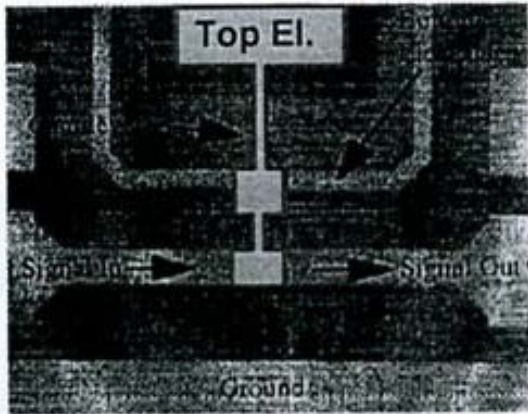
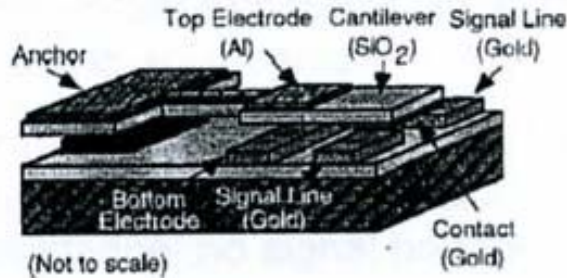- **Series-switch**
  - Structure
  - Fabrication
  - Performance

  - Ex. of **contact-switches** →

Cantilever beam with electrostatic actuation

J.J. Yao, M.F. Chang, Solid-State Sensors and Actuators, 1995 and Eurosensors IX, Transducers '95.

Switch architecture:
- suspended SiO_2 cantilever arm
- **platinum-to-gold electrical contact**
- electrostatic actuation

Performance:
- DC to RF range of frequency
- $R_{DC}=0.22\Omega$
- Pull in voltage=28V, max current=200mA
- speed: $30\mu s$
- **-50dB isolation and 0.1dB insertion loss @ 4GHz**
- monolithic integration with IC because of the low temperature budget of the process
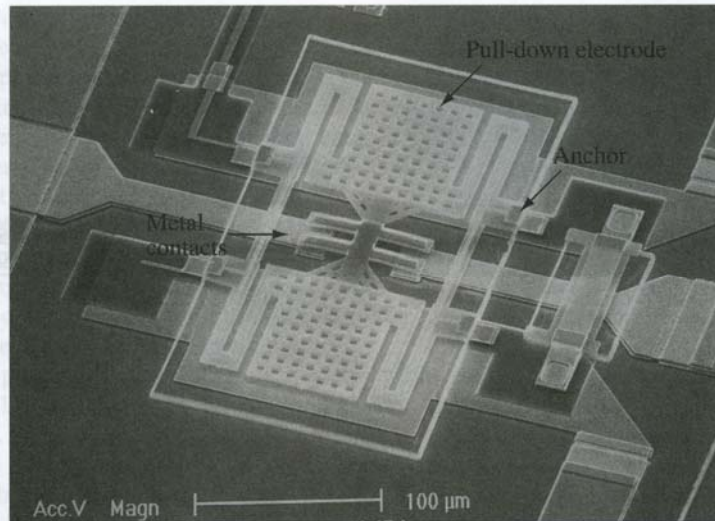
44

Rockwell series-switch

Figure 5.8. SEM of the Rockwell Scientific MEMS series switch [24] (Copyright IEEE).
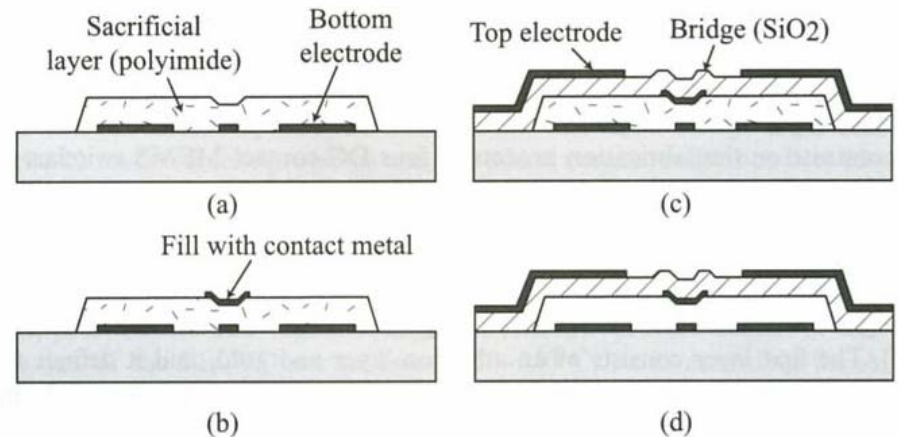
Sketch of principle

Figure 6.6. The fabrication process of the Rockwell Scientific series switch [8, 9].

Rebeiz

Rockwell series-switch, contd.

TABLE 5.6. Parameters for the Rockwell Scientific DC-Contact MEMS Series Switch

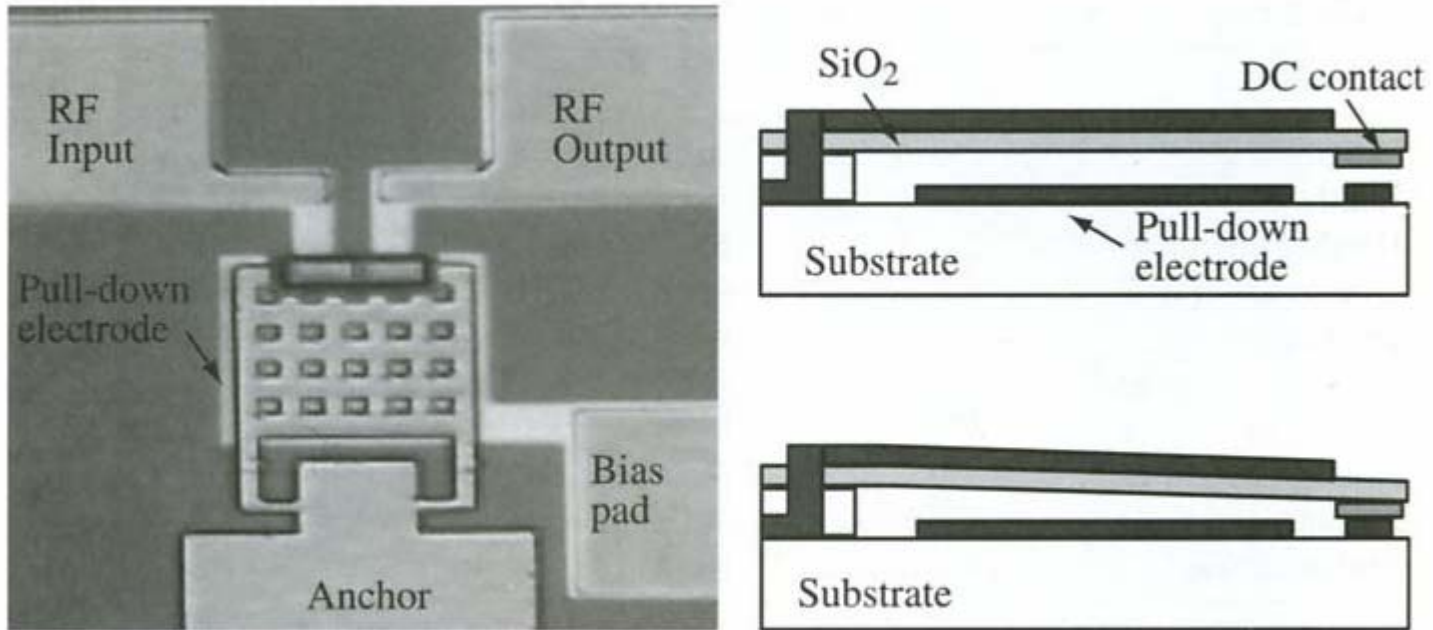| Parameter	Value	Parameter	Value
Length [μm]	250	Actuation area [μm²]	75 × 75 (×2)
Width [μm]	150	Actuation voltage [V]	50–60
Height [μm]	2–2.5	Switch time [μs]	8–10
Cantilever type	Oxide, Au	Switch resistance [Ω]	0.8–2
Thickness [μm]	2, 0.25	C_u [fF]	1.75–2
Residual stress [MPa]	Low	Inductance [pH]	40–60
Spring constant [N/m]	15	Isolation [dB]	−50 (4 GHz)
Holes in cantilever	Yes	Isolation [dB]	−30 (40 GHz)
Sacrificial layer	Polyimide	Isolation [dB]	−20 (90 GHz)
Bridge release	Plasma etch	Loss [dB]	−0.1 (0.1–50 GHz)

Motorola

Figure 5.9. Photomicrograph of the Motorola DC-contact MEMS series switch and cross sections in the up- and down-state positions (Copyright IEEE).

Rebeiz

Motorola, contd.

TABLE 5.7. Parameters for the Motorola DC-Contact MEMS Series Switch

Parameter	Value	Parameter	Value
Length [μm]	140	Actuation area [μm^2]	100 × 80
Width [μm]	100	Actuation voltage [V]	40–60
Height [μm]	2–3	Switch time [μs]	2–4
Cantilever type	Oxide, Au	Switch resistance, R_s [Ω]	1–2
Thickness [μm]	1.3, 0.3	C_u [fF]	2
Residual stress [MPa]	Low	Inductance [pH]	20
Spring constant [N/m]	35–40	Isolation [dB]	−44 (2–4 GHz)
Holes in cantilever	Yes (8 μm)	Loss [dB]	−0.15 (0.1–6 GHz)
Sacrificial layer	Polyimide		
Bridge release	Plasma etch		

Rebeiz

Lincoln

Figure 5.12. SEM of the Lincoln Laboratory in-line DC-contact MEMS series switch [31] (Copyright IEEE).
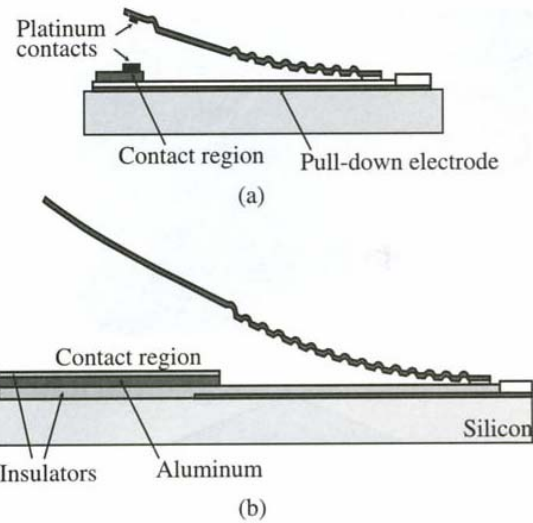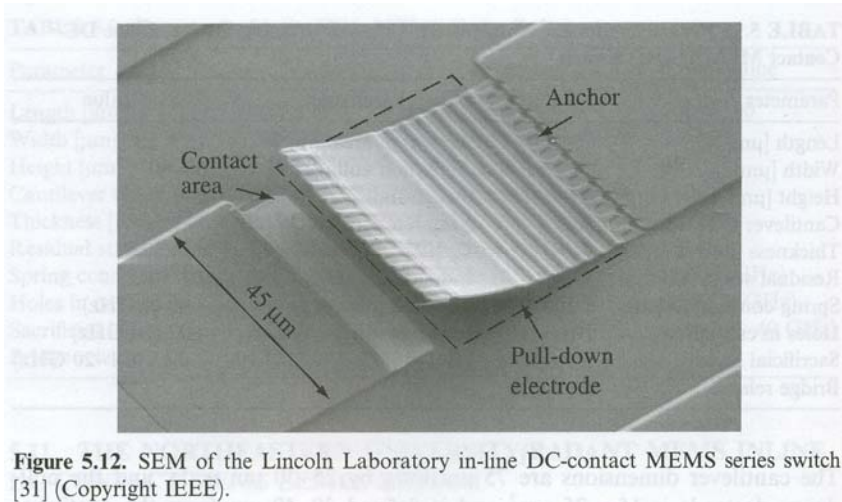

Figure 5.13. Cross section of the DC-contact (a) and capacitive-contact (b) Lincoln Laboratory inline switch (Copyright IEEE).

Lincoln, contd.

TABLE 5.10. Parameters for the Lincoln Laboratories Inline MEMS Series Switch

Parameter	Value	Parameter	Value
Length[a] [μm]	55/200	Actuation area [μm^2]	45 × 50
Width [μm]	50	Actuation voltage[b] [V]	30–80
Height [μm]	2–15	Switch time[b] [μs]	1–20
Cantilever type	Oxide, Al, oxide	Switch resistance, R_s [Ω]	1–2
Thickness [μm]	0.2, 0.5, 0.2	C_u [fF]	4–6
Residual stress	Very high	Inductance [pH]	Negligible
Holes in cantilever	No	Isolation [dB]	−40 (4 GHz)
Sacrificial layer	Polyimide	Isolation [dB]	−22 (30 GHz)
Bridge release	Freeze Drying	Loss [dB]	−0.15 (0.1–40 GHz)
Dielectric[c] (Å)	SiO$_2$ (1000)		

[a]Capacitive switch: 200 μm. DC-contact switch: 55 μm.
[b]Capacitive switch: 30–40 V and 20 μs; DC-contact switch: 60–80 V and <1 μs.
[c]Above pull-down electrode only.

Examples of implemented switches
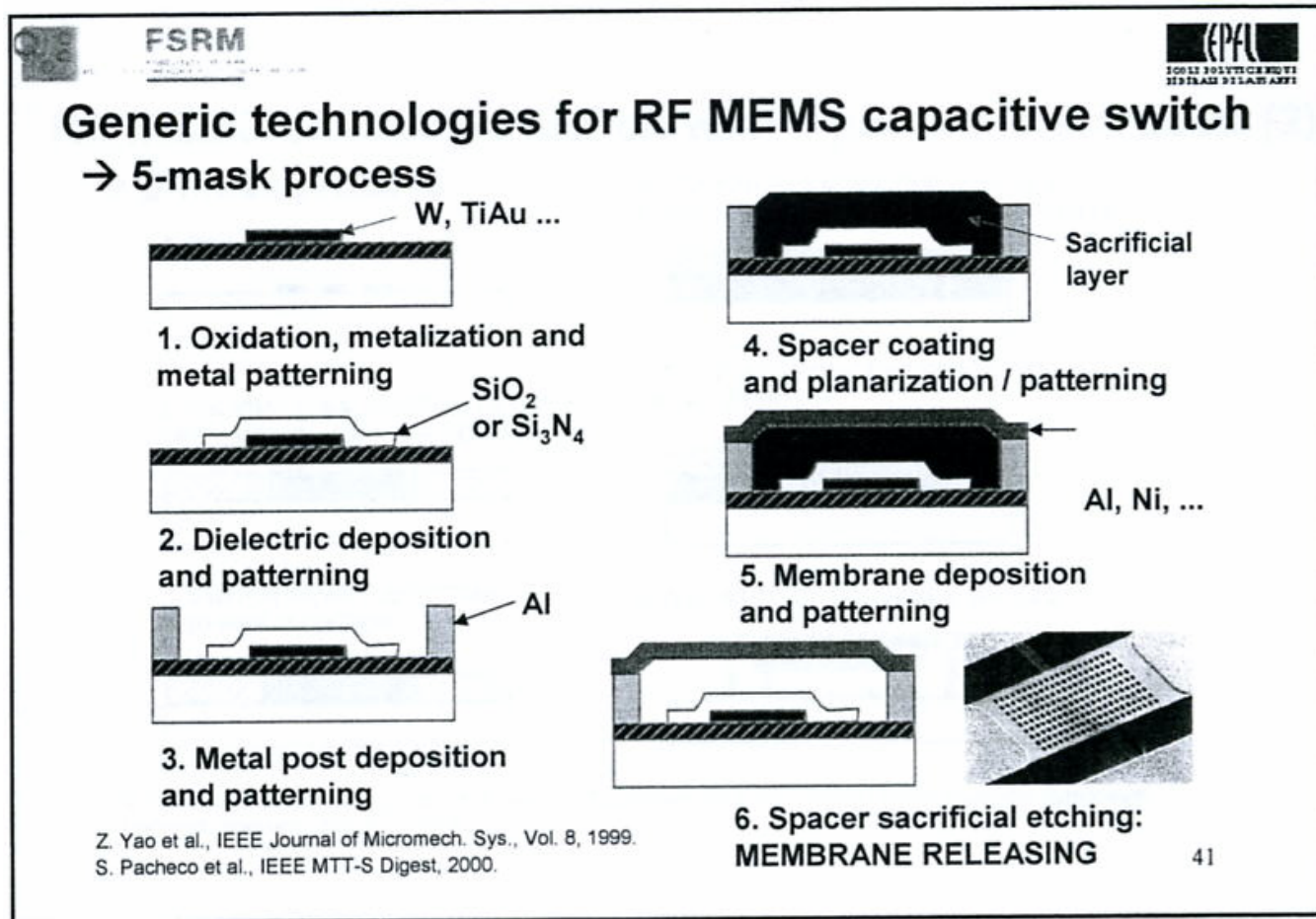
- **Shunt-switches**

  - Structure

  - Fabrication

  - Performance

  - Ex. of capacitive **shunt-switches** $\rightarrow$

Fabrication of capacitive switch

Generic technologies for RF MEMS capacitive switch

→ 5-mask process

1. Oxidation, metalization and metal patterning (W, TiAu ...)

2. Dielectric deposition and patterning (SiO$_2$ or Si$_3$N$_4$)

3. Metal post deposition and patterning (Al)

4. Spacer coating and planarization / patterning (Sacrificial layer)

5. Membrane deposition and patterning (Al, Ni, ...)

6. Spacer sacrificial etching: MEMBRANE RELEASING

Z. Yao et al., IEEE Journal of Micromech. Sys., Vol. 8, 1999.
S. Pacheco et al., IEEE MTT-S Digest, 2000.
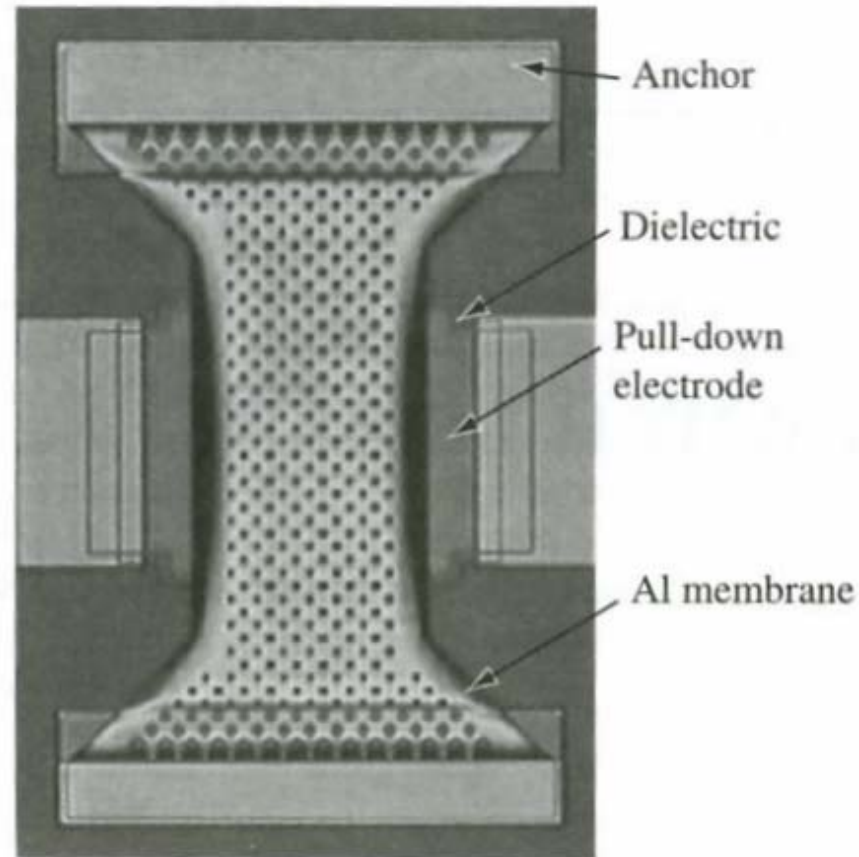
41

Raytheon

Figure 5.1. Photomicrograph of Raytheon MEMS capacitive shunt switch [2, 3] (Copyright IEEE).

Rebeiz

Raytheon, contd.

TABLE 5.1. Parameters for the Raytheon Capacitive MEMS Shunt Switch

Parameter	Value	Parameter	Value
Length [μm]	270–350	Actuation area [μm^2]	80 × 100
Width [μm]	50–200	Actuation voltage [V]	30–50
Height [μm]	3–5	Switch time [μs]	3/5 (D/U)
Membrane type	Aluminum	C_d [pF]	1–6
Thickness [μm]	0.5	Capacitive ratio	80–120
Residual stress [MPa]	10–20	Inductance [pH]	5–10
Spring constant [Nm]	6–20	Resistance [Ω]	0.25–0.35
Holes [μm]	Yes (3–5)	Isolation [dB]	−20 (10 GHz)
Sacrificial layer	Polyimide	Isolation [dB]	−35 (30 GHz)
Bridge release	Plasma etch	Intermodulation	+66 dBm
Dielectric (Å)	Si$_3$N$_4$ (1000)	Loss [dB]	−0.07 (10–40 GHz)
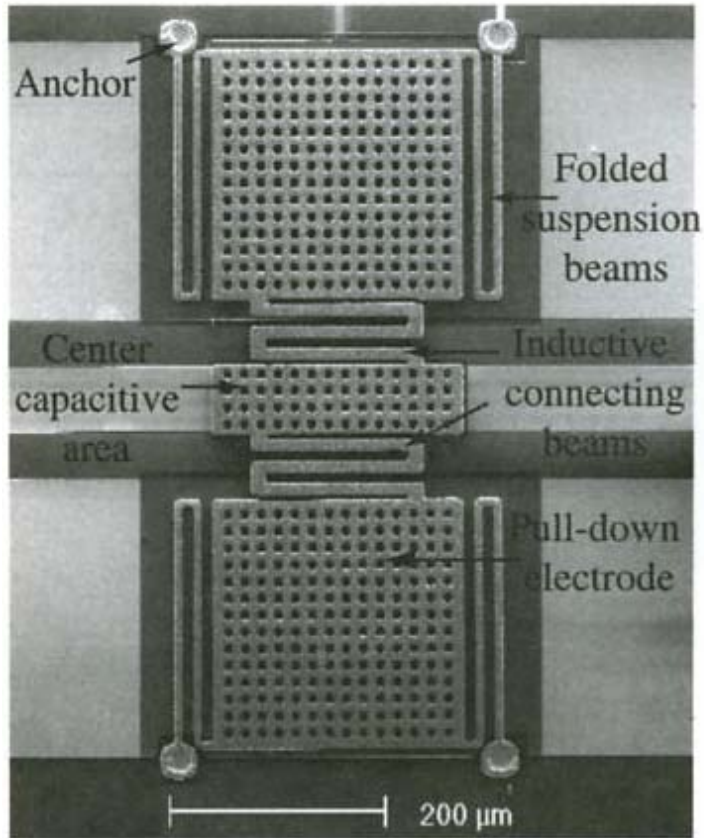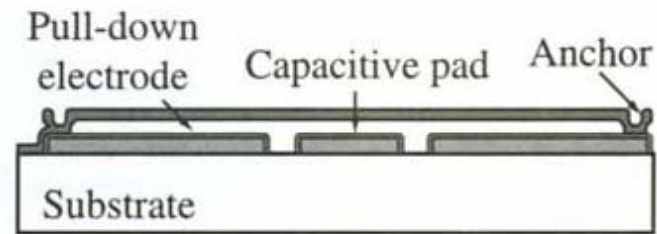
Rebeiz

Univ of Michigan

Figure 5.2. Photomicrograph of the university of Michigan low-voltage MEMS shunt switch. The number of meanders can be varied from 1 to 8 [7] (Copyright IEEE).
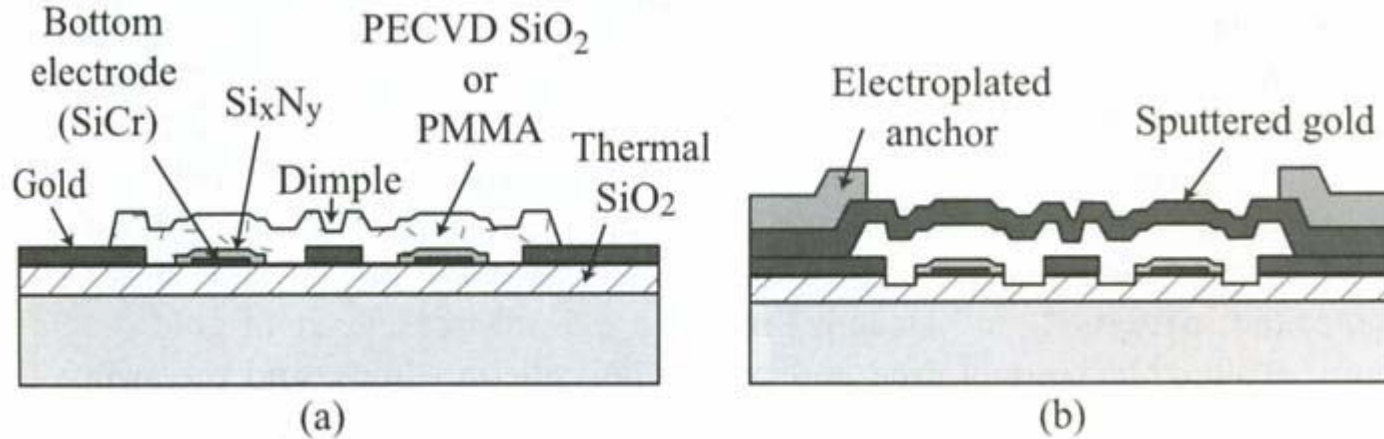
Rebeiz

Fabrication, "Michigan switch"

Figure 6.7. The fabrication process of the Michigan all-metal series switch [10, 11] (Copyright IEEE).

Rebeiz

Univ of Michigan

TABLE 5.2. Parameters for the University of Michigan Low-Voltage MEMS Capacitive Shunt Switch

Parameter	Value	Parameter	Value
Length [μm]	500–700	Actuation area [μm^2]	200×200 (×2)
Width [μm]	200–250	Actuation voltage[a] [V]	6–20
Height [μm]	4–5	Switch time[a] [μs]	20–40 (D)
Membrane type	Nickel	C_d [pF]	1–3
Thickness [μm]	2–2.5	Capacitive ratio	30–50
Residual stress [MPa]	20–100	Inductance [pH]	1–2
Spring constant [N/m]	1–10	Resistance [Ω]	0.2–0.3
Holes [μm]	Yes (10)	Isolation [dB]	−25 (30 GHz)
Sacrificial layer	Polyimide	Intermodulation	N/A
Bridge release	Plasma etch	Loss [dB]	−0.1 (1–40 GHz)
Dielectric (Å)	Si$_3$N$_4$ (1000–1500)		

[a]Depends on number of meander support.

Rebeiz

Special switch structures

- 3 electrodes can also be used
  - Top-electrode used to "clamp" the active electrode to the top
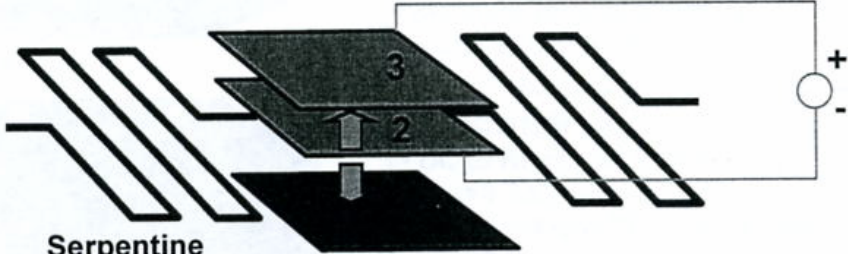 - Important for systems experiencing **large accelerations**

FSRM

RF MEMS capacitive switch with 3 parallel electrodes (1)

→ Architecture with 3rd electrode: avoid switch movements in acceleration gradients (airborne systems, > 10g!)
→ 2nd bias used to clamp the 'active' electrode to the top

Serpentine spring

S. Pacheco, C. T.-C. Nguyen, and L. P. B. Katehi, Proceedings, IEEE MTT-S International Microwave Symposium, Baltimore, Maryland, June 7-12, 1998.

42

Ionescu, EPFL

60

Liquid/metal contact-switch

- May solve reliability problem of solid state – solid state contacts
  - → Use **liquid-to-solid state**
- Mercury (Hg) is candidate due to good properties
    - Low contact resistance
    - No signal ringing
    - No contact degradation
  - Electrostatic actuation
    - Actuation voltage 100 – 150 V
  - → Liquid not accepted in IC-industry!

Mercury switch
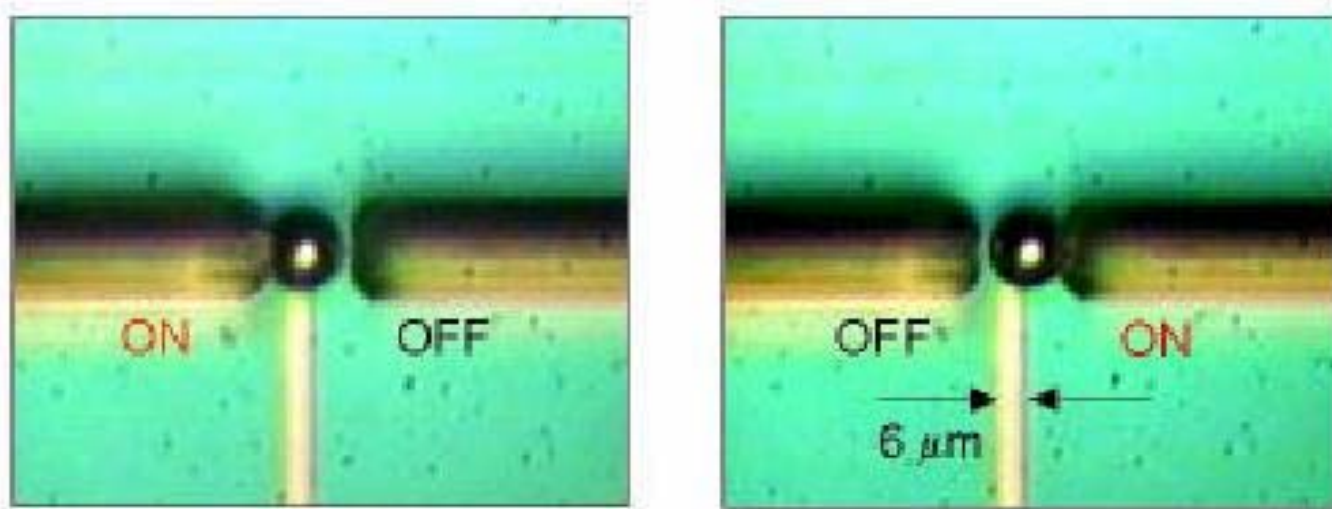
Mercury switch sphere moves

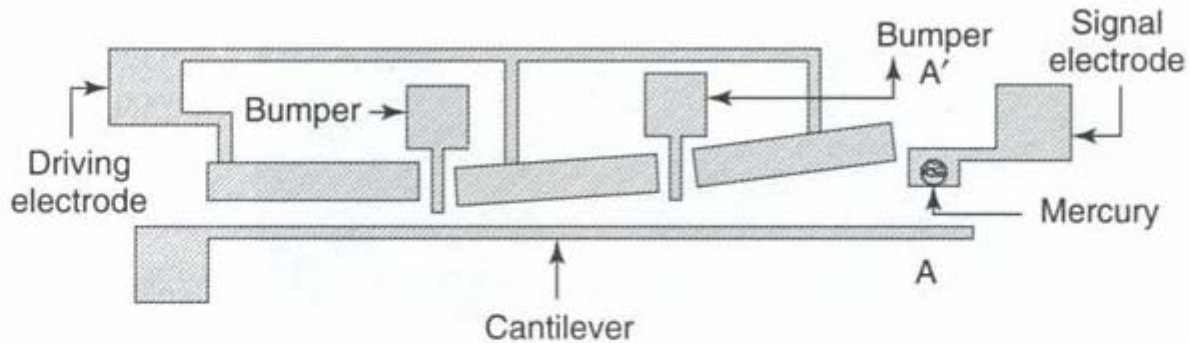Planar prosess, foto, JHU, Appl Physics Lab

Mercury switch

Figure 3.33 Schematic diagram of the mercury contact micro relay. Reproduced from S. Saffer, J. Simon and C.J. Kim, 1996, 'Mercury contact switching with gap-closing microcantilever', *Proceedings of SPIE*, 2882: 204–209, by permission of SPIE

Figure shows switch from above
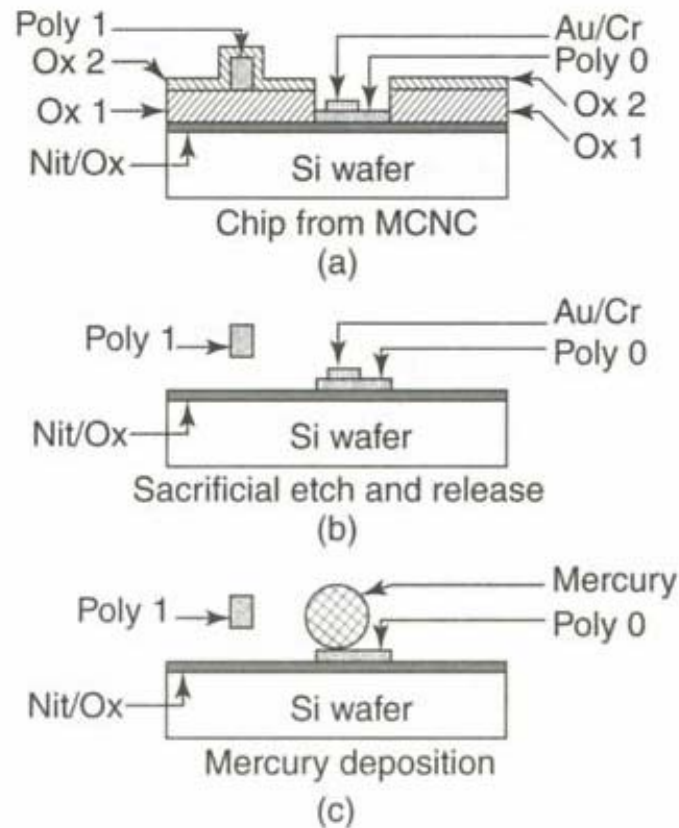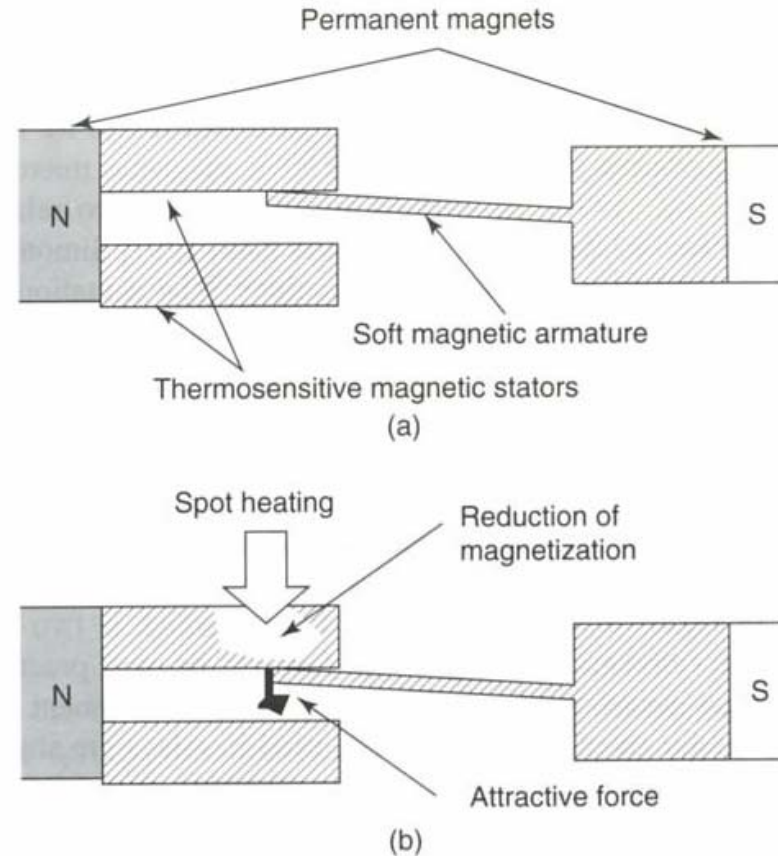
Varadan

63

Mercury switch, contd.

Figure 3.34 Process flow at cross-section AA' of Figure 3.33. Note: MCNC, Microelectronics Center of North Carolina. Reproduced from S. Saffer, J. Simon and C.J. Kim, 1996, 'Mercury contact switching with gap-closing microcantilever', *Proceedings of SPIE*, 2882: 204–209, by permission of SPIE

Varadan

Thermal actuation

Thermo sensitive magnets

Figure 3.38 Principle of operation of thermally controlled magnetization micro relay. (a) without heat; (b) with heat. Note: N, north; S, south. Reproduced from E. Hashimoto, H. Tanaka, Y. Suzuki, Y. Uensishi and A. Watabe, 1994, 'Thermally controlled magnetic actuator (TCMA) using thermo sensitive magnetic materials', in *Proceedings of IEEE Microelectromechanical Systems Workshop, 1994*, IEEE, Piscataway, NJ, USA: 108–113, by permission of IEEE, © 1994 IEEE

Varadan

65

Some challenges in switch design

- High electric field in small dimensions
  - Parts of metal surface may melt
  - Liquid metal damp conducts when switch is turned off
  - "Break-down" in dielectric

- Self actuation
  - If RF-signal modulates a DC voltage the beam can **self actuate**
    - May be beneficial to have **separate** pull-down electrodes

- Integration of switch with IC
  - (more on this in a future lecture)

Challenge: System-on-Chip (SoC)

Switch integrated on IC:

An Above IC MEMS RF Switch

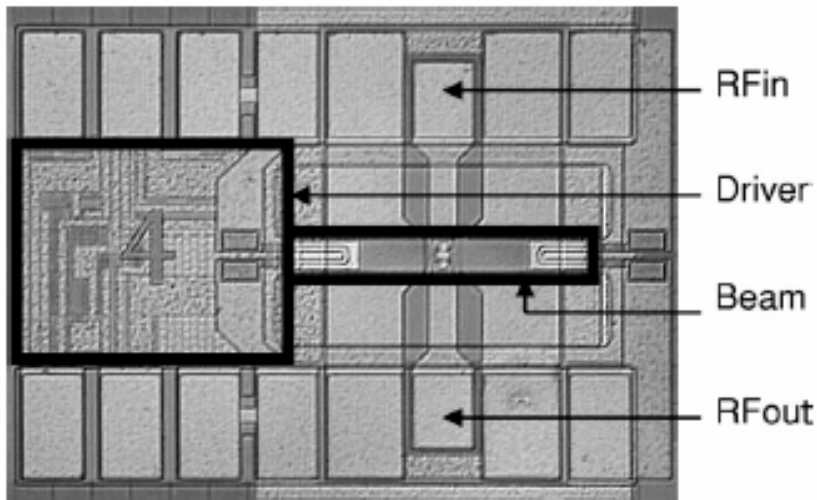Daniel Saias, Philippe Robert, Samuel Boret, Christophe Billard, Guillaume Bouche, Didier Belot, and Pascal Ancey
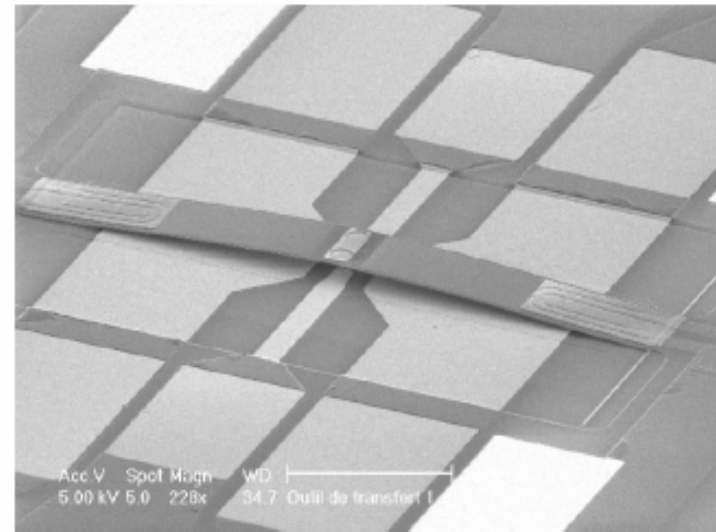
RFin

Driver

Beam

RFout

Fig. 9. Switch and driver die Micrograph.

Fig. 1. SEM view of the microswitch.

Saias et al, 2003

Comparing performance

TABLE II
RF SWITCHING DEVICES COMPARED PERFORMANCE

	FET switch [2]	SOI CMOS Tx/Rx Switch High Resistivity substrate [3]	Stand alone MEMS solution [4]	Integrated MEMS (this work)
Insertion Loss	2 @ 6GHz	0.7 @ 2.5GHz	0.15 @10GHz	0.4 @6GHz
Isolation (dB)	-20 @ 6GHz	-50 @ 2.5GHz	-15 @10GHz	-40 @6GHz
Rs series (Ohm)				2
Cup series (fF)				1
Size (um x um)	~1mm^2	0.02mm^2	120x280	300x900
Switching time	10ns	10ns	5.3us	~250us
Actuation	--	--	Electrostatic	Thermal + Electrostatic
Driver	--	--	External	Internal (300umx300um)
Integration	GaAs embedded	SOI design / Separate Chip	Separate chip	embedded

Saias et al, 2003